

Fast Neutrons Processes on Molybdenum Isotopes

C. Oprea, A.I. Oprea

*Joint Institute for Nuclear Research, Frank Laboratory of Neutron Physics,
Joliot-Curie 6, 141980 Dubna, Russian Federation*

Abstract. Molybdenum nucleus has many natural and artificial isotopes important for fundamental and applicative researches. Cross sections, angular correlations and isomer ratios in fast neutrons induced reactions up to 25-30 MeV were evaluated using codes realized by authors as well as dedicated software. Contributions of different nuclear reaction mechanisms in the cross sections were also determined. Parameters of nuclear optical potential, density levels and radius channels were extracted. Theoretical evaluations were compared with existing experimental data. The results of present work were realized in the frame of the fast neutrons scientific program at FLNP basic facilities (IREN and EG5) and are necessary for future experiment preparation.

INTRODUCTION

The Molybdenum nucleus, (protons numbers $Z=42$ and mass $A= 83-115$) has 33 isotopes of which 7 are natural ($A=92, 94, 95, 96, 98, 100$) and four isomers. The first 6 natural isotopes are stable but the nucleus with $A=100$ is unstable with the time of life of $7.8 \cdot 10^{18}$ y. The isotopes with $A=100$ is a fission product and it is used in medicine [1].

Nuclear reactions induced by fast neutrons are of great interest for fundamental and applicative researches. For fundamental investigations fast neutrons reactions are a source of new data on nuclear reactions mechanism and structure of nuclei. For applications these reactions provide precise nuclear data for reactors technology (fission and fusion), processing of long live nuclear waste, reprocessing of *U* and *Th* for transmutation and energy projects, accelerated driven systems (ADS) etc. [2–4]. Fast neutrons cross sections data for charged particles emission are of interest also because, the accumulation of Hydrogen and Helium in the walls and vessels of nuclear facilities lead to the modification of their physical properties [5].

Neutrons are neutral elementary particles and therefore they have high penetrability power in the matter. This property is very useful in neutrons activation analysis because it is possible to analyze large solid samples. Furthermore, the emitted gamma quanta resulted in the neutron capture process emerging from the samples can be also registered. Instrumental Neutron Activation Analysis (INAA) performed with slow neutrons is a powerful tool for elemental analysis. Complementary to INAA is Fast Neutrons Activation Analysis (FNAA) method which allows to obtain better gamma emitters [6].

The following reactions $^{94}\text{Mo}(n,p)^{94}\text{Nb}$ and $^{95}\text{Mo}(n,np)^{94}\text{Nb}$ induced by fast neutrons were analyzed. Cross sections, isomers ratios, parameters of nuclear optical potentials were also evaluated. The ^{94}Nb isotope can be found in the radioactive wastes. This nucleus is unstable, has a very large time of life ($T_{1/2} = 20300$ y) and contributes to the low level geological activity of the environment due the buried wastes [7, 8].

THEORETICAL BACKGROUND

Cross sections of $^{94}\text{Mo}(n,p)^{94}\text{Nb}$ and $^{95}\text{Mo}(n,np)^{94}\text{Nb}$ and of some concurrent processes which may influence the measurements were evaluated with Talys computer codes. In the calculations the contribution of all reactions mechanism (compound, direct and pre-equilibrium) were taken into account. In the case of compound processes the Hauser–

Feshbach approach of statistical model of nuclear reaction was considered [9]. Direct processes were described the Distorted Wave Born Approximation (DWBA) [10] and a two-component exciton model for pre-equilibrium processes was used [11].

Density levels were described by the constant temperature Fermi gas model [12]. The optical nuclear potential is of Woods–Saxon type, with real and imaginary part of volume, surface and spin-orbit components using locals and global parameters [13].

In the exit channels of mentioned reactions many isomer states are formed and from here it follows that will be of interest to evaluate in the experiment the corresponding isomer ratios. The expression of isomer ratio (neglecting the loss of charged particles in the target), used in the measurements, has the form:

$$R = Y_m \cdot Y_g^{-1} = \left(\int_{E_{thr}}^{E_{max}} N_0 \phi(E) \sigma_m(E) dE \right) \cdot \left(\int_{E_{thr}}^{E_{max}} N_0 \phi(E) \sigma_g(E) dE \right)^{-1} \quad (1)$$

where: $Y_{m,g}$ are the yields of isotope in isomer (m) and ground (g) states; N_0 is the number of nuclei in the target; ϕ is the flux of incident beam; $\sigma_{m,g}$ are the production cross section of m and g states respectively; E_{thr} is the threshold energy of emergent particle emission; E_{max} is the maximum energy of incident beam.

Talys is a freeware soft working under Linux, dedicated to nuclear reaction and structure of nuclei calculations with a friendly user interface. In these codes are implemented all models of nuclear reactions, density levels, optical potentials and related parameters to almost all nuclei and their isotopes. Parameters of Woods–Saxon nuclear potentials are obtained from processing of existing nuclear data for a large number of nuclei and isotopes. In the case when for some nuclides the parameters are not given then they are defined globally according with the approach described in [13]. Incident particles in Talys can be neutrons, protons, deuterons, tritium, 3He and alpha particles with energy up to 1000 MeV. This software is in development by free contribution of many users.

Talys gives the possibility to evaluate inclusive and exclusive cross sections. Lets consider a binary nuclear reaction of type $A(a,b)B$. The cross section is considered inclusive when in the final state are measured emergent “ b ” particle from all possible open channels. The exclusive cross section is characterized by the situation when particles in the emergent channel “ $b+B$ ” are in a well defined states of spin, parity, energy levels etc.

A comprehensive description of Talys, with models, formalisms and approaches, possibilities and limits can be found in codes documentation and reference [14].

RESULTS AND DISCUSSIONS

The ^{94}Nb isotope in isomer and ground states can be obtained in the $^{94}Mo(n,p)^{94}Nb$ and $^{95}Mo(n,np)^{94}Nb$ reactions for incident neutrons energy starting from emergent particles threshold up to 25 MeV. For both processes the cross sections and isomer ratios were evaluated. In the given incident neutrons energy range other channels are open. Some of them are concurring with the reactions of interest because they have the cross sections of the same order of magnitude. Inclusive and exclusive cross sections with default Talys input parameters of optical potential and levels’ density are evaluated. In the exit channels 10 discrete levels of residual nucleus were considered. The main properties of investigated reactions and of concurrent ones are given in the Table 1. The spin and parity of ^{94}Mo and ^{95}Mo in fundamental state are 0^+ and $(5/2)^+$ respectively.

Table 1. Q is heat of reaction; $J_{m,g}^{\Pi}$, $\tau_{m,g}$ are spin, parity and time of life of isomer and ground states; E_{γ} is gamma transition energy; 1, 3 – reaction of interest ; 2, 4 – concurrent reactions (M = main, C = concurrent)

	Reaction	$Q[\text{MeV}]$	J_m^{Π}	J_g^{Π}	τ_m	τ_g	$E_{\gamma}[\text{MeV}]$	Obs
1	$^{94}\text{Mo}(n,p)^{94}\text{Nb}$	-1.262	3^+	6^+	6.263 m	$2.03 \times 10^3 \text{ y}$	0.041	M
2	$^{94}\text{Mo}(n,np)^{93}\text{Nb}$	-8.49	$(1/2^-)$	$(9/2^+)$	16.13 y	stable	0.308	C
3	$^{95}\text{Mo}(n,np)^{94}\text{Nb}$	-8.631	3^+	6^+	6.263 m	$2.03 \times 10^3 \text{ y}$	0.041	M
4	$^{95}\text{Mo}(n,p)^{95}\text{Nb}$	-0.143	$(1/2^-)$	$(9/2^+)$	80.60 h	34.975 d	0.236	C

First the inclusive reactions stated in lines 1, 2, 3, 4 of Table 1 were evaluated. The contribution of all reaction mechanisms, given by discrete and continuum states of the residual nuclei are separated. In the Figure 1 are shown the results of inclusive reaction of $^{94}\text{Mo}(n,p)$ process.

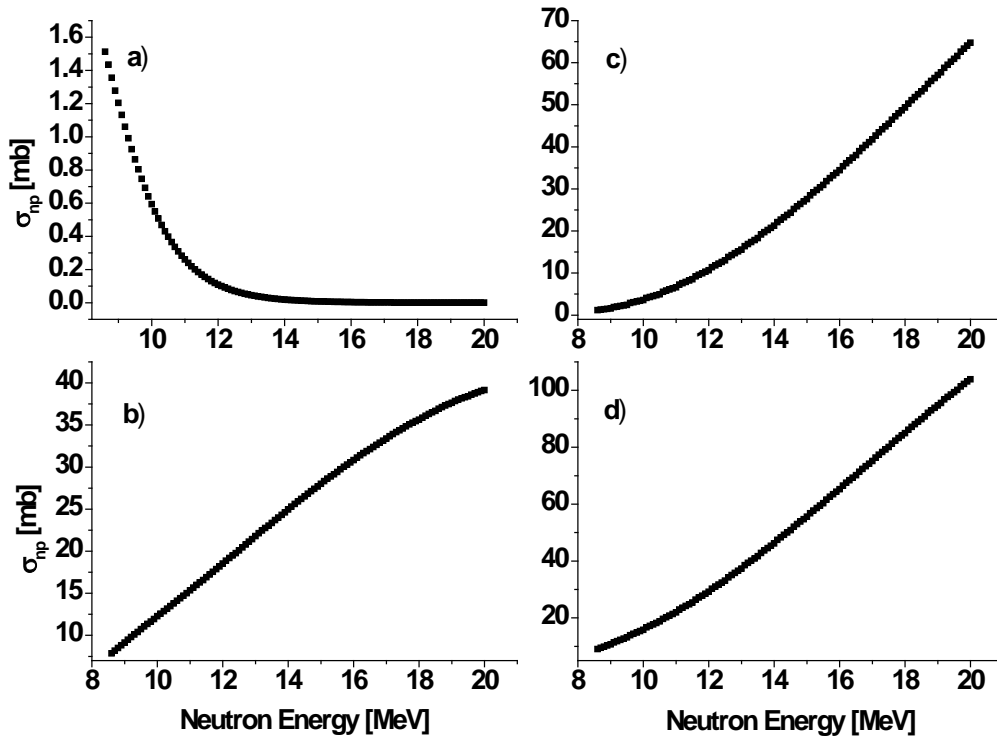


Figure 1. Inclusive cross section (XS) of $^{94}\text{Mo}(n,p)$ reaction. a) Compound processes on discrete states b) Compound on continuum c) Direct on continuum d) Total XS.

Discrete states, for both compound and direct processes have a very small influence on the cross sections in comparison with the continuum ones. The contribution to the cross section of compound processes on discrete states (shown in Fig.1a)) are with order of magnitude greater than the contribution of direct processes on discrete states and therefore the last are not represented in Fig.1. From Figs. 1b) and 1c) the main contribution to the cross section are given by continuum states of the residual nuclei and in the given incident neutron energy interval the compound and direct processes are of the same order of magnitude and competing with each other. The shape of the cross sections is in accordance with theory in each analyzed cases. At low energies the cross sections are increasing until to a maximum

value and followed after by a decreasing. From Fig. 1b) it is observing that the compound processes will reach the maximum faster than the direct ones (Fig. 1c)). From here results that the contribution of direct processes on the cross section are higher in comparison with compound processes and with the increasing of the energy the direct processes will become dominant. Talys calculations indicate that the compound and direct processes represented in Fig.1 are generated by the pre-equilibrium mechanism. In Fig. 1d) the total inclusive cross section for $^{94}\text{Mo}(n,p)$ reaction is represented taking into account all type of processes and states of residual nuclei. Same inclusive cross sections evaluations for all reactions from Table 1 are done but are not shown here. It is very interesting to mention that for all analyzed reactions from Table 1 there are the following common elements: the direct processes on continuum states of residual nuclei are higher in comparison with compound processes and the cross sections values have the same order of magnitude for all cases.

Production of ^{94}Nb nucleus in different states can be evaluated using exclusive cross sections. The results of $^{94}\text{Mo}(n,p)^{93m,g}\text{Nb}$ are represented in Fig. 2a). Cross sections of ground and isomer states production are designated by numbers 1) and 2). Total production of ^{94}Nb isotopes represented by the dependence 3, is compared with existing experimental data (Fig. 2a), curve 4) [15–17]. Description of experimental data, applying default Talys input can be considered satisfactory. Mainly the results on production of ^{41}Nb were obtained by activation methods, which are very difficult for elements with a very long time of life [15–17]. Furthermore, for neutrons energy up to 20 MeV many channels are open and they are in competition with the first analyzed reaction ($^{94}\text{Mo}(n,p)^{93m,g}\text{Nb}$) from Table 1. The following concurrent channels, $^{94}\text{Mo}(n,np)^{93}\text{Nb}$ (number 2 from Table 1) and $^{94}\text{Mo}(n,2n)^{93}\text{Mo}$ ($Q=-9.67$ MeV), must be taken into account for future measurements. In the Fig. 2.b. are represented the results for ^{93}Nb nucleus production in $^{94}\text{Mo}(n,np)^{93m,g}\text{Nb}$ reaction.

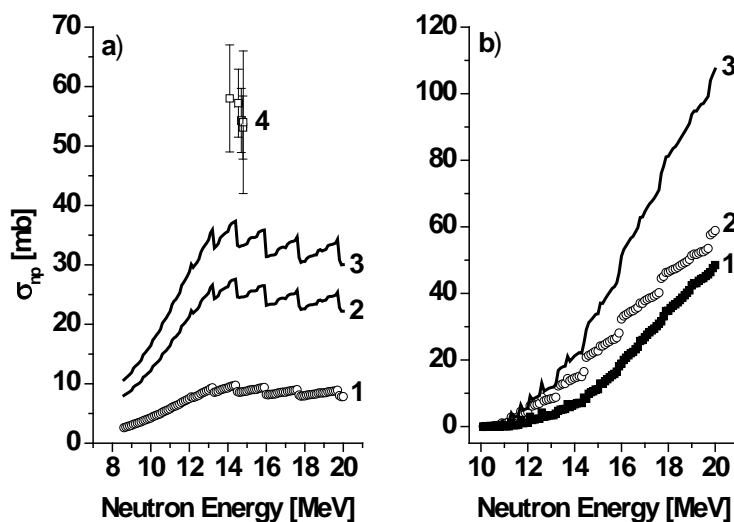


Figure 2. Exclusive XS. a) $^{94}\text{Mo}(n,p)^{93m,g}\text{Nb}$ for states: 1) ground, 2) isomer respectively, 3) total (1+2), 4) comparison with experimental data; b) $^{94}\text{Mo}(n,np)^{93m,g}\text{Nb}$ for 1) isomer, 2) ground, 3) total (1+2).

The cross section of (n,np) process from Fig. 2b) has a greater value than the (n,p) reaction from Fig. 2a) but however the authors had not found experimental data. In the given incident neutrons energy range it is difficult, in the measurements, to separate neutrons and protons of (n,np) process from neutrons and protons coming from other open channels.

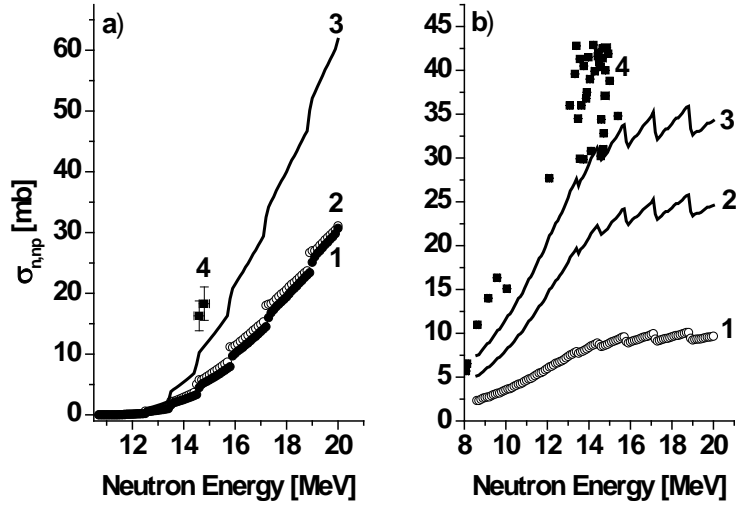


Figure 3. Exclusive XS. a) $^{95}\text{Mo}(n,np)^{94m,g}\text{Nb}$ reaction for 1) isomer, 2) ground, 3) total (1+2), 4) comparison with experimental data; b) $^{95}\text{Mo}(n,p)^{95m,g}\text{Nb}$ reaction for 1) isomer, 2) ground, 3) total (1+2), 4) comparison with experimental data.

The ^{94}Nb isotope can be obtained in $^{95}\text{Mo}(n,np)^{94}\text{Nb}$ reaction. Main properties of this process are shown in the row 3 of Table 1. For this reaction were evaluated also the inclusive cross section with a separation of different contribution of compound and direct processes on discrete and continuum states. Like in the case of $^{94}\text{Mo}(n,p)^{94}\text{Nb}$ reaction, the main contribution to the cross section is given by continuum states. Moreover, cross section given by direct processes are, higher than those of compound ones and both, direct and compound, are coming from pre-equilibrium mechanism. Inclusive processes for the $^{95}\text{Mo}(n,np)^{94}\text{Nb}$ and corresponding competing channels were not represented.

For $^{95}\text{Mo}(n,np)^{94}\text{Nb}$ process also were considered possible competing channels and they are: $^{95}\text{Mo}(n,p)^{95}\text{Nb}$ (number 4 from Table 1) and $^{95}\text{Mo}(n,2np)^{93}\text{Nb}$ ($Q=-15.857\text{ MeV}$). In the Figure 3.a. are shown the cross section production of the reaction of interest $^{95}\text{Mo}(n,np)^{94}\text{Nb}$. In the Figure 3b) exclusive cross sections of $^{95}\text{Mo}(n,p)^{95}\text{Nb}$ concurrent process are represented also. The results of other competing process are not given because their cross sections are lower and the threshold particle production is higher than in the investigated cases.

Fig. 3a) shows the experimental data taken from [15]. In Fig. 3b) are represented experimental data in a wide energy interval up 16–18 MeV [15, 18, 19]. Experimental data follows qualitatively the theoretical evaluations and a satisfactory agreement can be considered. The cross sections of investigated reaction (Fig. 3a)) and of competing process (Fig. 3b)) are of the same order of magnitude and must be considered in future measurements. Taking into account the theoretical values of isomer and ground states production and the satisfactory agreement between theory and experiment it is possible to evaluate the isomer ratios of the processes from Fig. 2 and Fig. 3 using relation (1). Two types of neutrons sources were considered. In the first case has the flux is equal with unity. In the second case the flux is much closer to reality and is proportional with $1/E^{0.9}$ (E is the neutron energy) like in the case of pulsed neutrons sources like IREN and IBR2 reactor from LNF. Results of evaluated isomer ratios for all reactions from Table 1 are given in Table 2.

Table 2. Isomer ratios obtained for investigated (I) and concurrent (C) processes in the case of neutrons source with incident flux 1) $\phi = I$; 2) $\phi \sim 1/E^{0.9}$; $E_\gamma =$ gamma transition energy

	Reaction	E_γ [MeV]	$R_1 \pm \Delta R_1$	$R_2 \pm \Delta R_2$	Obs
1	$^{94}\text{Mo}(n,p)^{94}\text{Nb}$	0.041	2.852 ± 0.013	2.860 ± 0.013	I
2	$^{94}\text{Mo}(n,np)^{93}\text{Nb}$	0.308	1.426 ± 0.015	1.511 ± 0.025	C
3	$^{95}\text{Mo}(n,np)^{94}\text{Nb}$	0.041	0.927 ± 0.019	0.923 ± 0.018	I
4	$^{95}\text{Mo}(n,p)^{95}\text{Nb}$	0.236	0.402 ± 0.025	0.393 ± 0.028	C

The neutron energy interval taken into account in the evaluation of isomer ratios is starting from about 8 MeV up to 20 MeV. The R values are very close in the both cases, but the absolute error ΔR is higher in the second case, because with the increasing of the energy the number of incident neutrons is slowly decreasing. In the relations (1) it is necessary to calculate the integrals. Cross sections were evaluated numerically with a step of 0.1 MeV and therefore the integrals are approximated by sums, which are the origin of absolute errors ΔR .

All calculations of cross sections and isomer ratios are done with default Talys input of Woods–Saxon (WS) potential parameters and densities states. In the Table 3 are extracted optical potential parameters that are influencing in a higher degree the cross sections.

Table 3. WS parameters. Real and imaginary VWS. Real SO. V , W , V_{SO} = potential depth; r = radius; a = diffuseness; Channel (row): 1), 3) incident and 2), 4) emergent

	Channel	Volume WS (VWS)						Spin Orbit (SO)		
		Real Part			Imaginary Part			Real Part		
		V [MeV]	r_v [fm]	a_v [fm]	W [MeV]	r_w [fm]	a_w [fm]	V_{SO} [MeV]	r_{SO} [fm]	a_{SO} [fm]
1	$n+^{94}\text{Mo}$	50.99	1.22	0.658	0.16	1.22	0.658	5.99	1.05	0.58
2	$p+^{94}\text{Nb}$	61.94	1.21	0.664	0.13	1.21	0.664	6.03	1.041	0.59
3	$n+^{95}\text{Mo}$	51.27	1.21	0.664	0.16	1.21	0.664	5.99	1.044	0.59
4	$p+^{94}\text{Nb}$	62.10	1.21	0.664	0.13	1.21	0.664	6.03	1.044	0.59

The evaluations have demonstrated that the most significant part of potential is the VWS parameters with real and imaginary part. In a lower degree the cross sections are influenced by the real part of SO components. The imaginary part of SO potential depth is taken zero in the default Talys calculations. The surface and other parameters of WS components are not shown here. The extracted parameters have the values in the general accepted range of magnitude.

CONCLUSIONS

Cross sections, isomer ratios and activities, of the nuclear processes indicated in the Table 1 were evaluated. Inclusive and exclusive cross sections were obtained with Talys computer codes using the default parameters input. From inclusive cross sections, the contributions of each nuclear-reaction mechanism on discrete and continuum states of residuals nuclei were obtained. For the given incident neutrons energy interval the direct processes, coming from pre-equilibrium mechanism, are giving the main contribution to the cross sections.

Exclusive cross sections allow to calculate the production of an isotope in a well defined states and therefore isomer ratios for different pairs of isomer – ground states were obtained.

For many presented theoretical results on cross sections and isomer ratios in the nuclear reactions with fast neutrons on *Mo* isotopes there are no experimental data. There will be of interest for fundamental and applicative researches to plan some future measurements for obtaining new nuclear data.

The present work is a part of nuclear data and isotopes production programs realized at IREN and IBR2 facilities of LNF JINR Dubna.

Acknowledgement. The work was supported by Cooperation Program between JINR Dubna and Romanian Research Institutes coordinated by JINR Dubna Plenipotentiary Representative of 2018–2019 years and FLNP Thematic Plan.

REFERENCES

1. J. Meija, T.B. Coplen, M. Berglund, W.A. Brand, P.D. Bièvre, M. Gröning, N.E. Holden, J. Irrgeher, R.D. Loss, T. Walczyk, T. Prohaska, *Pure Appl. Chem.*, **88**(3), (2016) 265–291.
2. M. Salvatores, I. Slessarev, A. Tchistiakov, *Nucl. Sci. Eng. P.*, **130**, (1998) 309–319.
3. M. Salvatores, A. Zaetta, C. Girard, M. Delpech, I. Slessarev, J. Tomassi, *Appl. Radiat. Isot.*, **46** (6), (1995) 681–687.
4. C. Rubbia, J. A. Rubio, S. Buono, F. Carmine, N. Fieter, J. Galvez, C. Geles, Y. Kadi, R. Klapisch, P. Mandrillon, J.P. Revol, and C. Roche, Report CERN/AT/95-44(ET) (1995); [http://cern.web.cern.ch/CERN/Divisions/SL/EER/Energy Amplifier/PDF/95-44.pdf](http://cern.web.cern.ch/CERN/Divisions/SL/EER/Energy%20Amplifier/PDF/95-44.pdf)
5. G. Khuukhenkhuu, Yu.M. Gledenov, M.V. Sedysheva, M. Odsuren, J. Munkhsaikhan, T. Delgersaikhan, *Journal Physics of Elementary Particles and Atomic Nuclei (PEPAN) Letters*, **11** (6), (2014) 1159–1168.
6. G. Berri, F. Mezzeti, A. Da Re, A. Bortolotti, L. Rapezzi, V.A. Grybkov, *Nucleonika*, **45** (3), (2000) 189–191.
7. Y. Ikeda, C. Konno, IAEA Vienna, INDC(NDS)-286, (1993), p. 27–31.
8. L. R. Greenwood, D. G. Doran, H. L. Heinisch, *Phys. Rev.*, **C 35** (1), (1987) 76.
9. W. Hauser, H. Feshbach, *Phys. Rev.*, **87**, 2, (1952) 366.
10. G.R. Satchler, *Direct Nuclear Reactions*, Oxford University Press, New York (1983).
11. A.J. Koning, M.C. Duijvestijn, *Nucl. Phys.*, **A 744**, (2004) 15.
12. Amos de Shalit, Herman Feshbach, *Theoretical Nuclear Physics*, John Wiley and Sons, ISBN13: 9780471203858 (1974).
13. A.J. Koning, J.P. Delaroche, *Nucl. Phys.*, **A 713**, (2003) 231.
14. A.J. Koning, S. Hilaire and M.C. Duijvestijn, TALYS-1.0., Proceedings of the International Conference on Nuclear Data for Science and Technology, April 22–27, 2007, Nice, France, editors O.Bersillon, F. Gunsing, E. Bauge, R. Jacqmin, S. Leray, EDP Sciences, (2008) 211.
15. L.R. Greenwood, D.G. Doran, H.L. Heinisch, *Phys. Rev.*, **C 35**, (1987) 76.
16. Y. Ikeda, C. Konno, A. Kumar, Y. Kasugai, IAEA Vienna, INDC(NDS)-342, (1996), 19.
17. Xiangzhong Kong, Yongchang Wang, Junquan Yuan, Jingkang Yang, *Journal of Radioanalytical and Nuclear Chemistry*, **V. 227**, (1998) 15.
18. P. Reimer, V. Avrigeanu, S.V. Chuvaev, A.A. Filatenkov, T. Glodariu, A. Koning, A.J. M. Plompen, S.M. Qaim, D.L. Smith, H. Weigmann, *Phys. Rev. C* **71**, (2005) 044617.